Bring Your Own Bow: Real-Time Bowing Parameter Estimation from String Sensor Data

Eoghan Ó Néill
eoneill65@qub.ac.uk
SARC: Centre for Interdisciplinary Research in Sound and Music
Belfast

Maarten van Walstijn
m.vanwalstijn@qub.ac.uk
SARC: Centre for Interdisciplinary Research in Sound and Music
Belfast

Miguel Ortiz
m.ortiz@qub.ac.uk
SARC: Centre for Interdisciplinary Research in Sound and Music
Belfast

Abstract

We present methods for real-time estimation of bowing force and bow velocity from a single bowed string using sensors located off-the-bow. Bow velocity is estimated from the voltage induced in the string as it moves through a fixed magnetic field at the bowing point. A histogram-based method is used to isolate the sticking phase of bowed-string motion, when bow and string move at the same velocity. Bowing force is estimated from reaction forces measured at the string supports using load cells.

The system is implemented on a compact monochord and provides robust estimates of bowing parameters. We describe the sensing hardware, signal processing, and calibration procedures, and evaluate the accuracy, limitations, and practical operating ranges of the proposed methods.

Real-time coupling of the estimated parameters to a bowed-mass physical model demonstrates their use as excitation signals for friction-driven physical models. The results indicate that these methods are well suited for the design of bowed virtual-acoustic instruments.

Keywords

bowing parameter estimation, interface design, virtual-acoustic instruments

1 Introduction

Bowing parameter estimation has been widely studied and is of interest across multiple research areas. In gestural analysis [1, 16, 18], playability studies [7, 8], and music pedagogy [11, 12, 15], bowing parameter estimates are commonly used to examine technique, physical effort, and skill development, and in musical instrument design, they most often serve as real-time control signals for sound synthesis [13, 19]. These applications place distinct and sometimes conflicting requirements on sensing methods, particularly with respect to measurement accuracy and precision, robustness, intrusion, and suitability for sustained musical interaction.

In this work, we use real-time bowing parameter estimates as control signals to excite bowed friction-driven physical models. This approach builds on the concept of virtual-acoustic instruments introduced by Mehes et al., in which excitation parameters are sensed from a control interface—designed to mirror the form and interaction of a traditional instrument—and mapped to a physical model [10]. This allows performers to apply established playing techniques to the excitation of physical models. For bowed-string models, bowing force and bow velocity are the primary excitation parameters governing energy transfer between bow and string [4]. Because bowing force and bow velocity correspond directly to performer-controlled parameters, estimates of these parameters from a control string can be mapped to a physical model, enabling a bowed virtual-acoustic instrument. This supports interaction through familiar bowing gestures, with haptic feedback provided by the control string and sonic feedback provided by the model.

This focus places specific constraints on how bowing parameters can be sensed. Estimation must be performed in real time, with sufficient robustness for use in performance contexts, and without imposing intrusive hardware on the performer. While sensing directly on the bow has been widely explored and is appropriate for many research goals [1, 5, 19], it poses challenges for instruments intended to investigate skill transfer. Added mass, altered balance, and changes in bow compliance affect playability and alter the physical interaction between player and instrument. Such changes necessitate adaptation to a bow with different mechanical properties, making it difficult to attribute observed performance behaviours to previously acquired bowing skill. Existing approaches that do not require a sensor-equipped bow rely on laboratory conditions that are incompatible with stage-ready instruments [8, 18].

In response to these constraints, we present off-the-bow sensing methodologies for estimating bowing parameters that are designed for real-time musical performance. Bowing force is estimated from load-cell measurements at the string supports, adapted from prior laboratory-based systems to operate on a compact monochord suitable for instrument development [6, 7]. Bow velocity is estimated indirectly from local measurements of string velocity at the bowing point, obtained via an electromagnetic pickup arrangement in which the string's motion through a fixed magnetic field induces a voltage in the string [3, 14]. Sticking periods, during which the string moves with the bow, are then isolated from this velocity signal to obtain the bow velocity estimate. Together, these methods provide the excitation parameters required to drive bowed friction-driven physical models while leaving the performer's bow unaltered.

Elements of the bowing force estimation approach were introduced in our prior work, where they were demonstrated within a playable bowed-string interface, alongside a preliminary offline exploration of bow velocity estimation [13]. The present paper extends this work by developing these methods into a real-time performance-oriented system, and empirically evaluating their limitations and practical operating regions. By demonstrating how these bowing parameter estimates can be coupled to a friction-driven physical model, the work provides a foundation for both the design of bowed virtual-acoustic instruments and the study of performer–instrument interaction in real-time musical interfaces.

NIME '26, June 23 - 26, 2026, London, UK

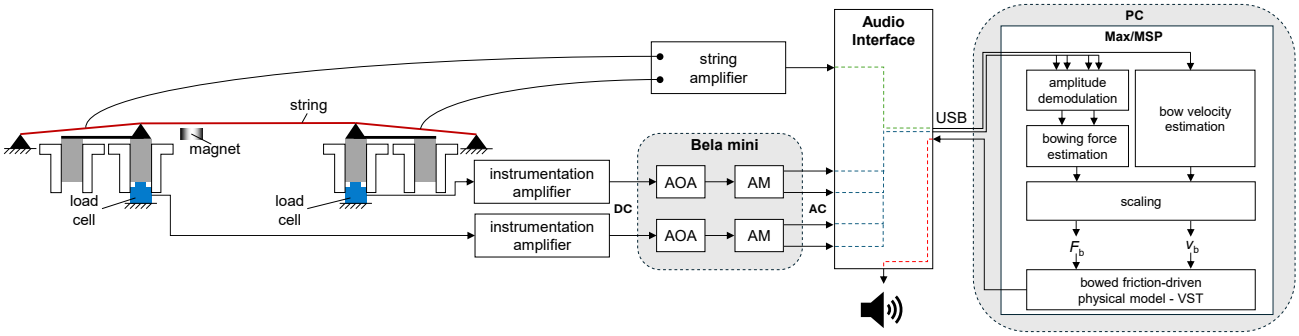

Figure 1: Bowing parameter estimation system schematic, showing the bowed-string interface, sensor placement, and signal processing.

2 Methodology

Figure 1 illustrates the overall structure of the proposed sensing system for bowing parameter estimation, including the bowed-string interface, sensor placement, and the subsequent signal processing and routing.

2.1 Bowing Force Estimation

Rather than measuring force directly on the bow, the method employed here estimates bowing force by inference from the reaction forces transmitted through the string to its fixed supports. When a string is bowed, the force applied by the bow is balanced by forces at the string supports—what on a traditional bowed string instrument would be the bridge and the nut. By measuring these reaction forces using load cells mounted beneath both of the string's supports, it is possible to estimate the applied bowing force. This follows directly from our prior work [13], which in turn builds on the work of Lampis et al. [6, 7].

This approach to bowing force estimation informed the design of the experimental monochord illustrated in Figure 1. Each end of the string is mechanically coupled to a single-axis load cell via a guided shaft assembly that constrains motion to the direction normal to the string. A secondary guided shaft is employed to prevent rotational motion of the load-cell-coupled shaft, ensuring consistent coupling between the string support and the load cell. This ensures that changes in the measured force correspond primarily to the normal component of bowing force, while maintaining a rigid and repeatable mechanical interface between string and sensor. The configuration presented here was previously reported in our prior work [13].

The load cells operate on the Wheatstone bridge principle and produce millivolt-range differential voltages proportional to the applied force, which are amplified using instrumentation amplifiers for real-time processing. Using load cells provides DC-coupled force measurements, allowing slow changes in bow pressure and subtle force variations to be captured.

In practice, the bowing force estimation precision is influenced by factors such as string tension, sensor drift, and mechanical tolerances. To maintain stable operation during extended performance, an automatic offset adjustment algorithm is employed to compensate for slow sensor output drift or changes in string equilibrium. This allows the system to remain responsive without requiring frequent recalibration. In the implementation presented here, the automatic offset adjustment is performed on a Bela Mini, and the resulting signals are amplitude modulated for transmission at audio rate to Max/MSP, as shown in Figure 1. Additional implementation details and early exploration of this algorithm are described in our prior work [13].

The resulting bowing force estimate obtained after demodulation is subject to a high noise level due to the limited signal-to-noise ratio achievable with the selected load cells and instrumentation amplifiers. To mitigate this, the estimate is processed using a first-order low-pass filter with a cut-off frequency of 10 Hz, chosen specifically to reduce noise while avoiding the introduction of excessive latency.

2.1.1 Calibration of Bowing Force Estimation. To convert the load cell voltage measurements into physical force units, a calibration procedure is required that accounts for the geometry and mechanical constraints of the monochord.

Our prior work presented a force calibration approach carried out on a 20 cm string, using a cradle to suspend known weights from the string at various positions [13]. The present interface employs a shorter 10 cm string within a more compact monochord. Although the underlying calibration procedure remains unchanged, the reduced spacing between the string supports prevents the use of the original cradle. To achieve reproducible loading in this constrained geometry, a custom 3D-printed hook is used to apply weights at the midpoint of the string. The hook features lateral guides that match the spacing between the linear ball bushings constraining the string supports, ensuring consistent positioning and symmetric force distribution. A small embedded magnet holds the weights securely without introducing additional mechanical constraints.

During calibration, incremental masses of 0 g, 100 g, and 200 g are applied sequentially, and the corresponding steady-state load-cell outputs are recorded after transient settling. Although the measured response is near-linear, small but systematic deviations from linearity are observed. These are attributed to a combination of mechanical compliance in the guided assemblies, load cell nonidealities, and geometric effects arising from string deflection. Consequently, a smooth non-linear scaling curve is fitted to the measured data and used to convert raw sensor output into an estimated bowing force during operation.

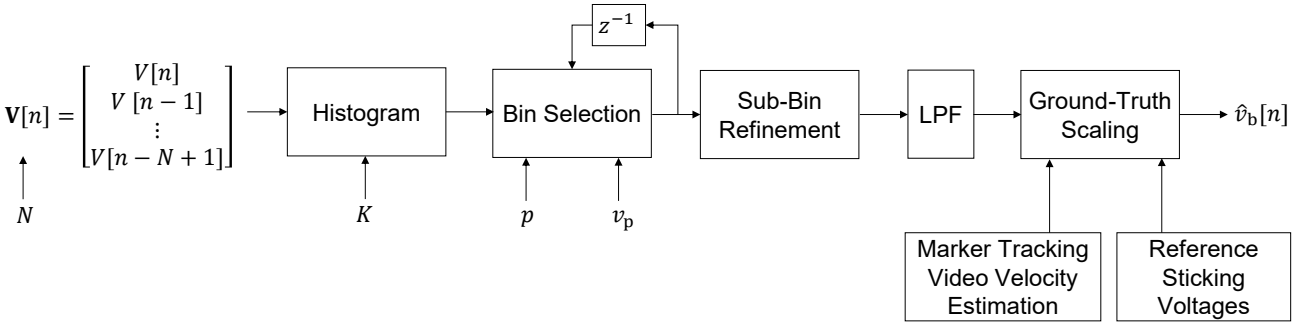

Figure 2: Histogram-based bow velocity estimation block diagram.

2.2 Bow Velocity Estimation

2.2.1 Stick-Slip. The estimation of bow velocity relies on stick–slip motion of the bowed-string. During bowing, the string alternates between periods of sticking to the bow hairs, moving at the same velocity as the bow, and slipping across the bow hairs in the opposite direction to the bow's motion. By isolating the string's velocity during sticking periods, the bow velocity can be inferred.

This approach is not restricted to the Helmholtz regime and applies across bowing conditions in which sticking periods statistically dominate the string velocity signal. However, the Helmholtz case provides a particularly transparent analytical example. In this regime, the relative bowing position r_b determines how the Helmholtz period P is divided between these phases. Apart from when bowing takes place at the midpoint of the string ($r_b = 0.5$), the sticking phase occupies a larger fraction of the period than the slipping phase. This relationship can be expressed as follows:

$$P_{\text{stick}} = \max(r_b,\ 1 - r_b)\, P$$

When bowing near one of the string supports, the sticking phase persists for most of the signal duration, enabling more reliable algorithmic isolation. Therefore, this methodology requires bowing to be performed close to one of the string supports. Informal testing further indicated that this positional dependence persists in a range of non-Helmholtzian bowing conditions, where excitation near a string support enabled more reliable isolation of the sticking phase.

The effectiveness of this estimation also depends on measuring string velocity close to the bowing position, as velocity along the string varies due to wave propagation and string dynamics. A sensor located near the bowing point captures string velocity most representative of the bow's motion; measurements taken further away degrade estimation accuracy.

2.2.2 String Velocity Sensing. Inspired by the "StringAmp" pickup system[1] as used in the works of Buys et al. [3] and Pardue et al. [14], string velocity is captured using a magnetically induced voltage. As shown in Figure 1, a permanent magnet is placed beneath the string so that its magnetic field is perpendicular to the string's length. As the string moves perpendicular to both its length and the magnetic field, a voltage is induced proportional to the local string velocity. This small voltage is amplified through a low-noise op-amp circuit to produce a signal suitable for processing.

2.2.3 Histogram-Based Bow Velocity Estimation. Bow velocity is estimated using a histogram mode extraction method, operating on a sliding circular buffer of length N, containing induced string voltage samples $\mathbf{V}[m]$ as illustrated in Figure 2. The buffer is updated sample by sample, with one new sample entering and one oldest sample leaving at each iteration, providing continuous, sample-by-sample estimates.

At each sample instant, the histogram is updated incrementally: one count is added to the bin corresponding to the new sample, and one count is removed from the bin corresponding to the sample exiting the buffer. The parameter K determines the number of bins spanning a fixed voltage range, which is normalised to [-1, 1], as the histogram is evaluated on audio samples whose amplitudes are bounded to this interval. Each histogram bin is assigned a score that combines two factors:

- Population score: reflecting the number of samples falling within the bin.
- Proximity score: reflecting how close the bin is to the previously selected bin, weighted by a user-defined factor p that adjusts the influence of continuity on the final bin selection.

The bin with the highest combined score is selected as representing the dominant sticking-phase voltage. The proximity factor p is dynamically scaled by a factor that ramps linearly from 1 to 0 over the interval $[-v_p, v_p]$. Within this range, p is gradually reduced to zero, while outside the interval the scaling factor is 1, leaving p unchanged. This is because the proximity score is less informative near zero, where the sticking and slipping velocity modes are very close in value and magnitude. As the modes begin to diverge from one another and leave this region, the proximity weighting could cause the method to mistakenly track the slipping mode instead of the dominant sticking mode, resulting in an incorrect estimate.

To achieve sub-bin resolution, we empirically developed a neighbour-weighted mode refinement. Denoting the population counts of the bins immediately below and above the selected bin by A and B, respectively, the estimated mode location is displaced within the selected bin by a fraction $A/(A + B)$ of the bin width. This heuristic was chosen based on experimental evaluation to reduce step-like behaviour arising from discrete bin selection and to produce smoother estimates than simple bin-centre assignment. Quadratic interpolation using the centre of the selected bin and the centres of its adjacent bins was also evaluated, but in our tests it produced less smooth results than the proposed neighbour-weighted refinement. In cases where the selected bin corresponds to the central, near-zero bin, the output is set to zero to suppress spurious estimates caused by overlapping sticking and slipping samples.

[1] produced by MusikLab Danemark, http://www.stringamp.com

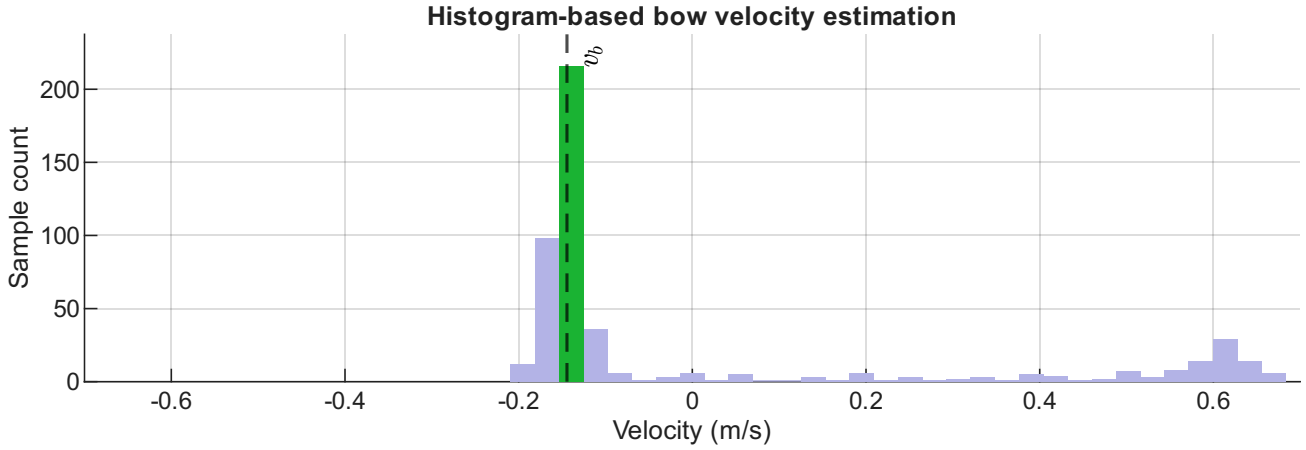

Figure 3: Example of bow velocity estimation histogram for a buffer length of 500 samples. The green bin denotes the selected bin. Note the presence of the slipping velocity mode around 0.6 m/s

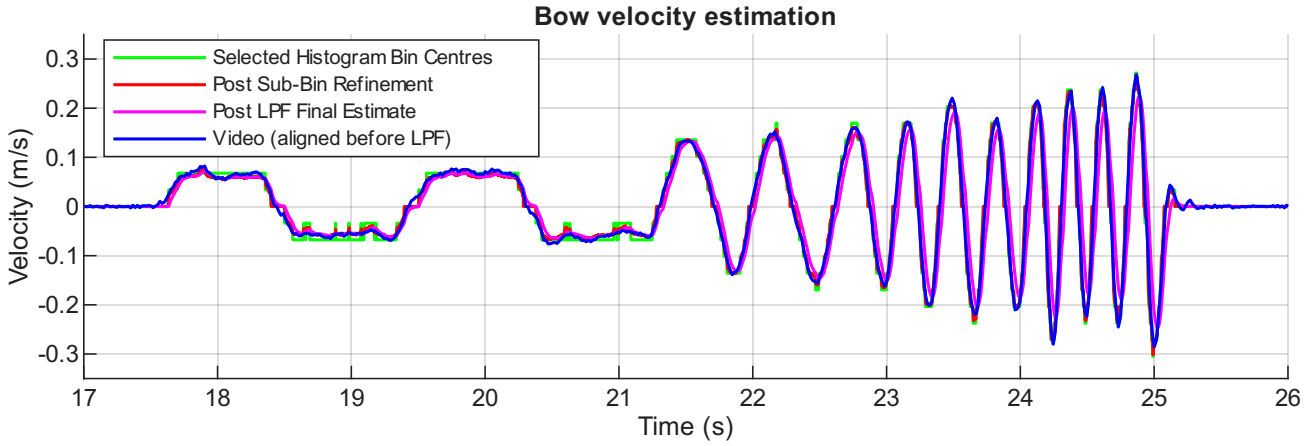

Figure 4: Bow velocity estimates at successive stages: discrete bin-centre, neighbour-weighted sub-bin refinement, and low-pass filtered output, compared with video-based reference measurements.

To improve continuity and suppress small artifacts, a first-order low-pass filter with a cut-off frequency of 10 Hz is applied to the histogram-derived sticking-phase voltage. This serves two purposes: first, during changes in bowing direction, the underlying sticking component passes through zero, a region in which sub-bin refinement cannot operate and the estimate may unnaturally flatline, producing discontinuities; second, the histogram-based method can occasionally select a bin slightly offset from the true dominant sticking component, resulting in brief discontinuities in the output. The low-pass filter mitigates both effects, yielding a smoother and more stable estimate.

Finally, to convert histogram-derived voltages into physical units, a reference bow velocity is obtained via a controlled video-based calibration procedure. A coloured marker of known width is attached to the bow and tracked by a fixed camera, with a bowing guide rail ensuring a constant distance between the marker and the camera throughout bowing, as shown in Figure 5. This maintains a consistent pixel-to-length ratio, enabling accurate estimation of bow velocity from the marker trajectory. During this calibration, the string voltage is recorded simultaneously and processed by the histogram-based estimator to extract the corresponding sticking voltage. The reference bow velocity is then used to determine a scaling factor that maps the sticking voltage to physical string sticking velocity, and thus to bow velocity. Once established, this scaling allows subsequent bow velocity estimation to be performed using string velocity measurements alone, without reliance on video tracking.

Figure 4 illustrates the successive stages of the bow velocity estimation process. The discrete bin-centre estimate obtained directly from histogram mode selection is shown in green. The neighbour-weighted sub-bin refinement is shown in red, producing a continuous estimate between bin centres. The final smoothed estimate, obtained by first-order low-pass filtering, is shown in pink. For reference, the independently measured bow velocity obtained from video-based marker tracking during calibration is shown in blue. The figure demonstrates the progressive reduction of quantisation artefacts and discontinuities through sub-bin refinement and filtering, and the close correspondence between the final histogram-derived estimate and the video-based ground truth.

The histogram-based method with neighbour-weighted sub-bin refinement was compared directly with kernel density estimation (KDE) using video-based bow marker tracking data as

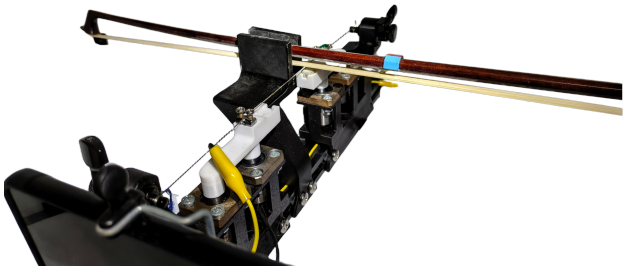

Figure 5: Bow tracking arrangement: sensing monochord with fixed mobile phone camera, bowing guide rail, and coloured marker on bow.

Figure 6: Sensing Monochord in Cello Orientation.

ground truth. The two approaches produced comparable accuracy and resolution in estimating the dominant sticking-phase voltage. The histogram method, however, has lower computational overhead, providing a simpler and more efficient option for real-time applications.

3 Coupling to a Bow-Mass Model

The estimated bowing parameters were used in real time to excite a friction-driven bow-mass physical model. Bow-mass models have been documented in the literature [2, 9]; while the specific bow-mass model implemented here has not been previously documented, it follows the same fundamental principles, providing a resonant mass whose motion is excited by bowing force and bow velocity. The bow–mass model is used here as a real-time test platform for evaluating the proposed off-the-bow parameter estimation framework, serving as an available real-time physical model for preliminary investigations while a real-time bowed-string model is under development.

For practical exploration of the interface, the third author, a cellist, performed bowing on the sensing monochord configured in a cello orientation, as shown in Figure 6. This arrangement allowed them to leverage learned bowing technique to excite the bow-mass model. The cellist was able to perceive the sound of the sensing string alongside the amplified output of the bow-mass model, although the latter dominated in volume. Figure 7 illustrates how the two bowing parameters were co-varied during three different bowing techniques. While the cellist had an understanding of the interface's design and sensing methodology, they had limited prior exposure to the constructed interface, spending approximately 20 minutes familiarising themselves with it before performing the bowing techniques presented here.

A notable feature of the bow–mass model is that variations in bowing force affect the duration of the sticking phase between the bow and the mass: increasing the bowing force prolongs sticking, lengthening the oscillation period and lowering the fundamental frequency of the resonant motion. While bowed strings show only subtle pitch flattening near the upper limit of stable stick-slip interaction [17], the bow–mass model exhibits this effect in a pronounced, exaggerated form. The corresponding changes in pitch are visible in the spectrogram of the model's output, shown in Figure 7.

During interaction with the model, the cellist modulated bowing force and bow velocity in response to haptic feedback from the sensing string and auditory feedback from the model, forming a closed-loop performer–instrument system. The independence of these feedback modalities introduced a perceptual mismatch that the cellist was required to negotiate in real time.

The cellist reported that, after a brief familiarisation period, they were able to negotiate the perceptual mismatch and apply their existing bowing techniques, as shown in Figure 7. Together, the recorded control signals and the performer's report suggest the feasibility of dynamic real-time control and support the use of the proposed off-the-bow estimation methods for actuating friction-driven virtual-acoustic instruments.

4 Discussion

4.1 Limitations and Constraints

A fundamental constraint of the proposed methodology is that to enable effective velocity sensing, bowing must occur near a string support and directly above the fixed magnet, as discussed in Section 2.2.1. In the current implementation, the string length is 10 cm, and the magnet is located 2 cm from one of the string supports. Reliable velocity estimates are generally obtained when bowing occurs between the magnet and the support, and up to approximately 2 cm away from the fixed magnet toward the string midpoint. Bowing outside this region reduces estimation accuracy because the sticking-phase velocity component becomes less dominant and wave propagation phenomena along the string increasingly influence the measured signal.

Despite this positional constraint, the current calibration procedure for the load-cell–based force measurement applies static loads only at the midpoint of the string. Physical constraints imposed by the load-cell assemblies and the placement of the fixed magnet prevent the application of known loads at other positions along the string. Consequently, the force estimation implicitly assumes that the relationship between applied transverse force and the measured reaction forces at the supports is independent of bowing position. Our prior analytical and experimental investigations indicate that this assumption is not strictly valid—as the point of force application approaches a support, the geometry of string deflection increases the proportion of the applied force projected onto the measured vertical reaction forces, producing a small systematic overestimation relative to the midpoint-based calibration [13]. Because reliable bow velocity estimation requires bowing near one of the string's supports, bowing necessarily occurs in a region where this overestimation is present. However, the error is small and consistent enough that we accept it as a practical trade-off: it permits a short and simple calibration procedure while providing bowing force estimates that remain stable, repeatable, and strongly correlated

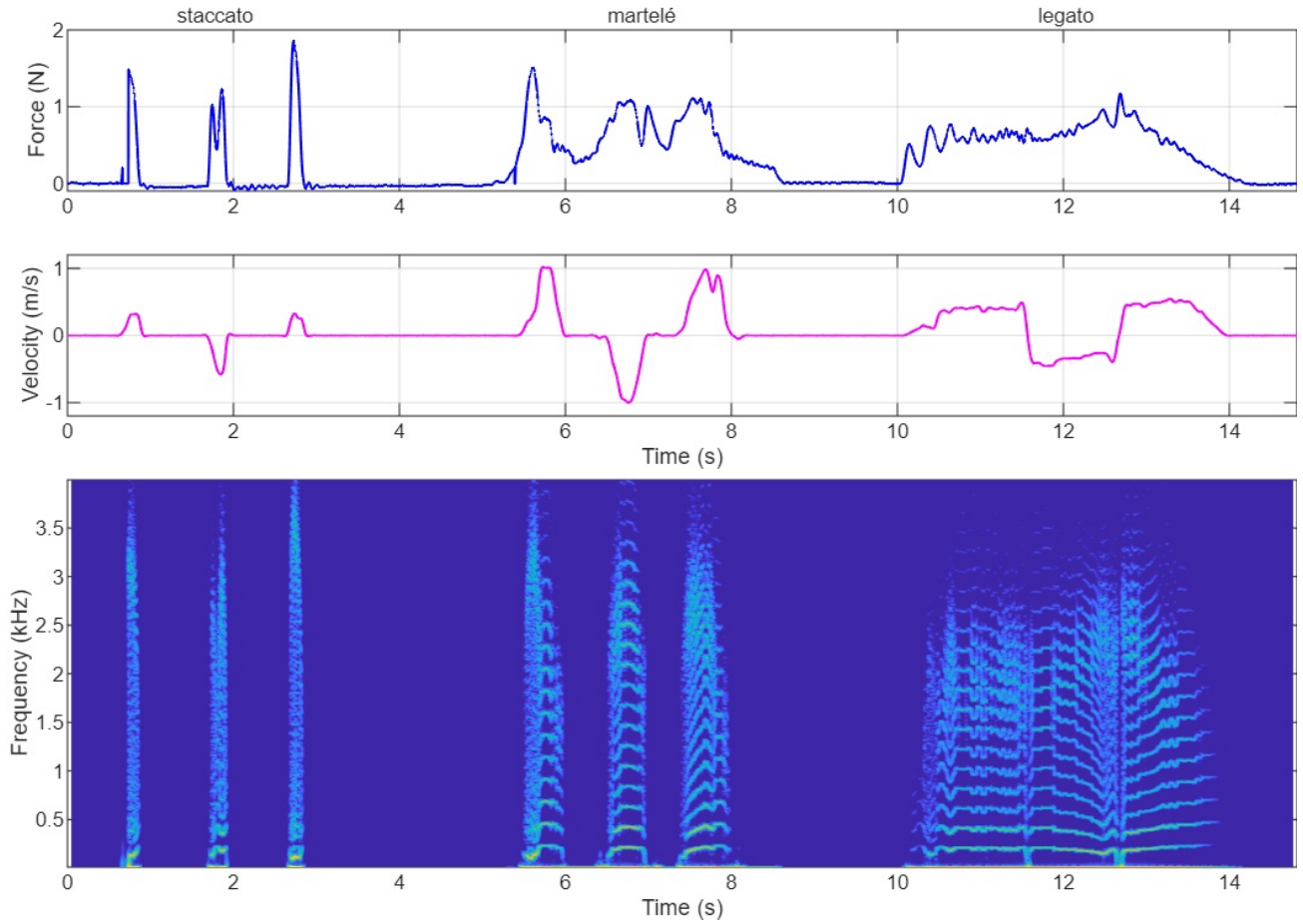

Figure 7: Estimated bowing force (top), estimated bow velocity (middle), and spectrogram of the bow–mass physical model's friction force output after high-pass filtering (bottom).

with performer intent, although they should not be interpreted as absolute measurements of bow–string contact force.

As shown in our prior work [13], bowing position can in principle be inferred from the relative outputs of the load cells. However, at low bowing forces the limited signal-to-noise ratio reduces the reliability of continuous position estimation, an effect that is particularly pronounced near the string supports where in this implementation bowing is to be constrained for the purposes of bow velocity estimation. For this reason, bowing position is employed as a supervisory signal rather than as a continuous control parameter. When the bow moves outside the reliable region near the magnet, the estimated bowing force can be progressively attenuated to prevent excitation of the physical model with poorly estimated bow velocity signals containing perceptually distracting artefacts. To ensure that the supervisory mechanism is engaged only when position estimation is reliable, the attenuation is activated above a minimum bowing force threshold. This design choice is specific to the combined bow velocity and bowing force estimation approach presented here, and ensures that the estimated parameters remain consistent with the performer's articulation.

4.2 Further Work

Planned future work includes a user study with experienced bowed-string players, in which the proposed interface is coupled to a state-of-the-art bowed-string physical model currently under development. This study will investigate the extent to which musicians trained on traditional bowed-string instruments can leverage their existing bowing skills to produce expressive and musically engaging interactions with virtual strings. By examining player adaptation and control fidelity, the study is envisioned to help evaluate the practical utility of the interface in realistic musical scenarios and inform further refinements to both hardware design and signal processing.

Besides this planned study, several avenues for further investigation remain. In particular, more systematic exploration of how string length, pitch, and tension affect bow velocity estimation would help clarify the operational limits and generality of the proposed methods. This includes testing a wider range of string lengths and thicknesses, as well as higher- and lower-capacity load cells, under controlled experimental conditions. Additional questions concern the mechanical design of the monochord: the current implementation uses 10 mm shafts and linear ball bushings at the supports. Extending the bowing force estimation method toward instrument design would likely require substantial mechanical redesign and miniaturisation.

5 Conclusion

Methods for real-time estimation of bowing force and bow velocity from a single bowed string using off-the-bow sensors have been presented. Bowing force was inferred from reaction forces at the string supports, measured using load cells. Bow velocity was estimated by isolating the sticking-phase velocity from the string's motion, measured via the voltage induced in the string as it moved through the magnetic field produced by a fixed magnet positioned beneath the string.

The methods were implemented on a compact monochord and evaluated with respect to calibration, limitations, and practical operating regions. Bow velocity estimation proved reliable when bowing near a string support and above the fixed magnet, where the sticking phase dominates the measured signal. Bowing force estimation, despite some position-dependent calibration error, produced stable, repeatable signals that reflect performer intent within this constrained bowing region. These estimates are supported by a position-aware attenuation mechanism that reduces excitation outside the reliable sensing region, ensuring robust and consistent real-time sensing of bowing parameters.

Coupling the estimated parameters to a bow-mass model demonstrated the feasibility of using the interface to drive friction-driven physical models. While the system does not achieve laboratory-level precision in measuring bowing parameters, it provides a balance between physical grounding and practical usability that aligns with the goals of new musical interface design.

Overall, the results indicate that these methods provide a viable foundation for the development of virtual-acoustic bowed instruments. By showing that these parameters can be estimated in real time and mapped directly to a friction-driven model without altering the performer's bow, this work marks an initial step toward designing interfaces that preserve familiar playing techniques. Future work will evaluate the interface with experienced bowed-string musicians to investigate control fidelity, player adaptation, and expressive potential.

6 Acknowledgements

The authors would like to thank Adam Schmidt, Laurel Pardue, and Andrew McPherson for helpful discussions and advice regarding string amplifier circuit design, and Alessio Lampis for insights related to load-cell interfacing. This research is supported by the Northern Ireland Department for the Economy (DFE).

7 Ethical Standards

This research did not involve human participants or animals.

References

[1] Frédéric Bevilacqua, Nicolas Rasamimanana, Emmanuel Fléty, Serge Lemouton, and Florence Baschet. 2006. The augmented violin project: Research, composition and performance report. In *Proc. of the 2006 International Conference on New Interfaces for Musical Expression NIME06.*

[2] Stefan Bilbao. 2009. *Numerical Sound Synthesis: Finite Difference Schemes and Simulation in Musical Acoustics.* John Wiley & Sons, Chichester. https://www.wiley.com/

[3] Kurijn Buys and Andrew McPherson. 2018. Real-time bowed string feature extraction for performance applications. In *Proc. of the 15th Sound and Music Computing Conference.*

[4] Matthias Demoucron. 2008. *On the control of virtual violins: physical modelling and control of bowed string instruments.* Ph. D. Dissertation. KTH Computer Science and Communication.

[5] Knut Guettler, Hans Wilmers, and Victoria Johnson. 2008. Victoria Counts: A case study with electronic violin bow. In *Proc. of the 2008 International Conference on New Interfaces for Musical Expression NIME2008.*

[6] Allesio Lampis, Alexander Mayer, and Vasileios Chatziioannou. 2024. Assessing playability limits of bowed-string transients using experimental measurements. *Acta Acustica* 8 (September 2024).

[7] Alessio Lampis, Alexander Mayer, Montserrat Pàmies-Vilà, and Vasileios Chatziioannou. 2023. Examination of the static and dynamic bridge force components of a bowed string. In *Proc. of Meetings on Acoustics.*

[8] Esteban Maestre, Jordi Bonada, Merlijn Blaauw, Alfonso Perez, and Enric Guaus. 2007. Acquisition of violin instrumental gestures using a commercial EMF tracking device. In *Proc. of the International Computer Music Conference.*

[9] Ewa Matusiak, Vasileios Chatziioannou, and Maarten Van Walstijn. 2025. Numerical modelling of elasto-plastic friction in bow–string interaction with guaranteed passivity. *Frontiers in Signal Processing* 5 (2025), 1525044. doi:10.3389/frsip.2025.1525044

[10] Sandor Mehes, Maarten van Walstijn, and Paul Stapleton. 2016. Towards a Virtual-Acoustic String Instrument. In *Proc. of the 13th Sound and Music Computing Conference (SMC2016).*

[11] Yurina Mizuho, Riku Kitamura, and Yuta Sugiura. 2023. Estimation of Violin Bow Pressure Using Photo-Reflective Sensors. In *Proc. of the International Conference on Multimodal Interaction.*

[12] Yurina Mizuho and Yuta Sugiura. 2024. A Comparison of Violin Bowing Pressure and Position among Expert Players and Beginners. In *Proc. of the 6th International Conference AsiaHaptics.*

[13] Eoghan Ó Néill, Maarten Van Walstijn, and Miguel Ortiz. 2025. Real-time bowing parameter sensing methods for articulated bow-string physical modelling. In *11th Convention of the European Acoustics Association—Forum Acusticum 2025: Proceedings.*

[14] Laurel S Pardue, Kurijn Buys, Michael Edinger, Dan Overholt, and Andrew P McPherson. 2019. Separating sound from source: sonic transformation of the violin through electrodynamic pickups and acoustic actuation. In *Proc. of the International Conference on New Interfaces for Musical Expression.*

[15] Laurel S. Pardue, Christopher Harte, and Andrew P. McPherson. 2015. A Low-Cost Real-Time Tracking System for Violin. *Journal of New Music Research* 44, 4 (Oct. 2015), 305–323. doi:10.1080/09298215.2015.1087575

[16] Erwin Schoonderwaldt. 2009. The player and the bowed string: Coordination of bowing parameters in violin and viola performance. *The Journal of the Acoustical Society of America* 126, 5 (2009), 2709–2720. doi:10.1121/1.3203209 Received 17 Mar 2009; Revised 6 Jul 2009; Accepted 7 Jul 2009.

[17] Erwin Schoonderwaldt. 2009. The Violinist's Sound Palette: Spectral Centroid, Pitch Flattening and Anomalous Low Frequencies. *Acta Acustica united with Acustica* 95, 5 (2009), 901–914. doi:10.3813/AAA.918221

[18] Erwin Schoonderwaldt and Matthias Demoucron. 2009. Extraction of bowing parameters from violin performance combining motion capture and sensors. *The Journal of the Acoustical Society of America* 126, 5 (November 2009), 2695–2708. doi:10.1121/1.3227640

[19] Diana Young. 2007. *A methodology for investigation of bowed string performance through measurement of violin bowing technique.* Ph. D. Dissertation. Massachusetts Institute of Technology.